

Waveform Analysis of Microwave Pulses Emitted in Association with Hypervelocity Impacts

Shigeo CHIBA¹, Eriko SOMA², Tadashi TAKANO^{1,3}

¹ Department of Electronics Engineering, School of Engineering, The University of Tokyo
7-3-1 Hongo, Bunkyo-ku, Tokyo, 113-8656, Japan, chiba@radionet.isas.jaxa.jp

² Department of Electrical Engineering, the Graduate School of Engineering, Tokyo University of Science
1-3 Kagurazaka, Shinjuku-ku, Tokyo, 162-8601, Japan, soma@radionet.isas.jaxa.jp

³ Institute of Space and Astronautical Science, Japan Aerospace Exploration Agency (ISAS/JAXA)
3-1-1 Yoshino-dai, Sagami-hara 229-8510, Japan, ttakano@radionet.isas.jaxa.jp

ABSTRACT

Formerly, microwave emissions accompanying hypervelocity impacts were confirmed experimentally. In this paper, two kinds of analyses, output waveform analysis and spectral analysis, are discussed for the purpose of clarifying the mechanism of microwave emissions. In output waveform analysis, the microwave pulse is simulated on the basis of a microcrack model in consideration of discharge current, and is compared with the experimental pulse in terms of the pulse shape. In spectral analysis, the amplitude and phase of the waveform is calculated in frequency domain to examine the characteristics of emissions. It is indicated that the spectral amplitude is nearly flat and the phase has coherency.

1. INTRODUCTION

In space, more than 10 million space debris are wandering the satellite orbit at the high speed of several km/s. They have a potential to give serious damage to spacecrafts. In relation to space debris, microwave emissions accompanying hypervelocity impacts were confirmed by experiments using an accelerator in the ground [1]. However, the mechanism of microwave emissions is not clear yet.

Until now, the microcrack model was proposed as the one of mechanism [2]. But it is not accomplished to show the validity of this model. In addition, although plasma particles appear at the time of the collision, it is thought that they don't contribute to microwave emissions [3]. So, it is also important to examine the characteristics of microwave pulses.

In this paper, two kinds of analyses, output waveform analysis and spectral analysis, are discussed in order to advance the clarification of mechanism. In output waveform analysis, the microwave pulse is simulated by means of numerical calculation on the basis of the microcrack model. And the analytical waveform is compared with the experimental one in terms of the pulse width and the shape to show the validity of the model. In spectral analysis, the complex spectrum of an experimental pulse is numerically calculated. The amplitude and the phase are discussed to show the characteristics of emissions and the difference between emissions due to this phenomenon and plasma particles.

2. A HYPERVELOCITY IMPACT EXPERIMENT

A. The experimental system

The experimental system including an accelerator is shown in Fig.1. The accelerator is a dual-stage light-gas accelerator. The projectile is spherical nylon of 7mm in diameter and the mass is about 0.2g. The target is aluminum, 15mm thickness and placed within the vacuum chamber. The degree of vacuum is about 0.2torr. A wire is installed in a zig-zag manner so as to make a plane vertical to the arrival directions of the projectile in front of the target and the observation trigger is generated when the wire is cut off by the projectile. Antennas are placed near side-on windows of the vacuum chamber to observe microwave emissions. The impact time is estimated by means of the projectile's speed measured by X-ray and the distance between the target and the wire.

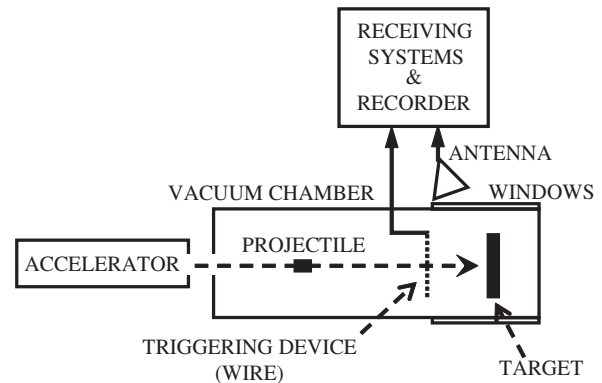


Fig. 1: The experimental system.

B. Receiving systems

Observation frequency bands of microwave emissions are 2GHz and 300MHz band. Firstly the receiving system for 2GHz band is explained. The system is configured as the heterodyne one as shown in Fig.2. The heterodyne system is used to convert RF (Radio Frequency) band into IF (Intermediate Frequency) one and obtain signals with adequately

lower frequency than the sampling frequency of recording apparatus. The receiving antenna is dipole antenna. LNA (Low Noise Amplifier) is installed to improve the measurement sensitivity of the received microwave. BPF is attached to narrow the frequency band. Mixer is installed to convert the frequency. The local oscillating frequency f_{LO} is configured as the out-of-band frequency of receiving system. Signals are amplified by IF Amp. and put into the recording apparatus. The recording apparatus is digital oscillo scope with the sampling frequency of 4GHz and the measurement time of 1000 μ s. At 300MHz band, the helical antenna and LNA, BPF are only used and the recording apparatus is installed without frequency conversion.

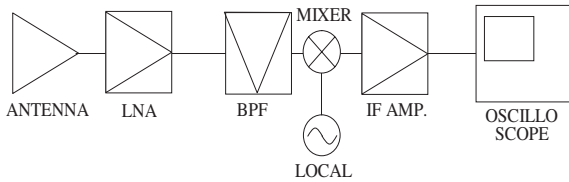


Fig. 2: The heterodyne receiving system for 2GHz band. The system for 300MHz band is composed of only antenna and LNA, BPF.

The frequency characteristics of receiving systems for 2GHz and 300MHz band are shown in Fig.3(a) and Fig.3(b), respectively. At 2GHz band, RF band defined as spectrum space of 3dB relaxation is 1850-2110MHz. Also, local frequency f_{LO} is configured as 2350MHz outside the RF band. Since local frequency f_{LO} is higher than RF band, frequency component of output waveforms is reversed. IF band is 1-1000MHz. At 300MHz band, RF band is 294-311MHz.

C. Experimental results

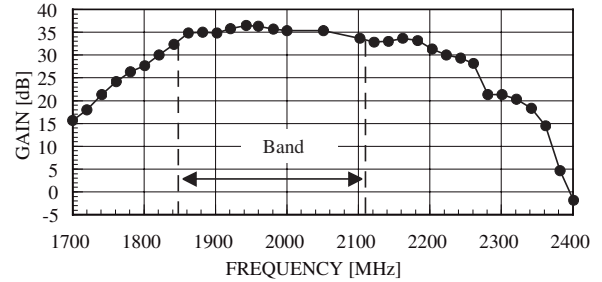
Experimental results at 2GHz and 300MHz band are shown in Fig.4 and Fig.5, respectively. The impact speed is 4.3km/s. The impact time is 58.1 μ s. At 2GHz band, a signal can be seen immediately after the impact. On the other hand, at 300MHz band, signals can be seen after several hundreds μ s of impact. In both frequency bands, waveforms are composed of a number of extremely-short pulses.

Expanded waveforms of arrowed pulses at 2GHz and 300MHz band are shown in Fig.4(b) and Fig.5(b), respectively. These pulses are extracted with the extraction time T_s . The extraction time T_s is 50ns at 2GHz band, 250 ns at 300MHz band, respectively.

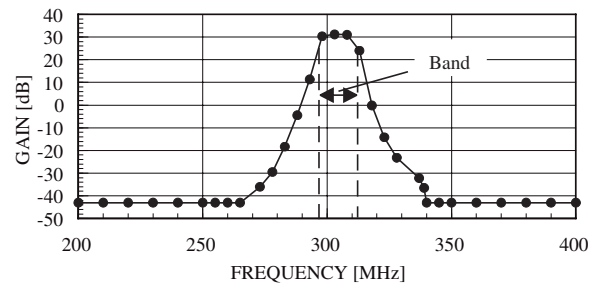
3. OUTPUT WAVEFORM ANALYSIS

A. The assumption of mechanism

We assume the microcrack model as the mechanism of microwave emissions. As shown in Fig.6, numerous small cracks called microcracks appear on the target at the time of the collision. On this occasion the charge is separated at the surface of microcrack, and the spark discharge current $i(t)$ flows across the microcrack. The microwave is emitted by the

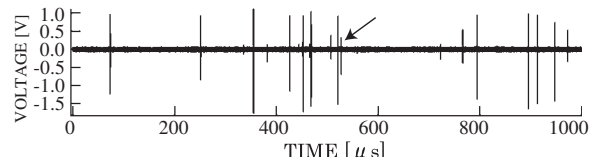


(a) 2GHz band.

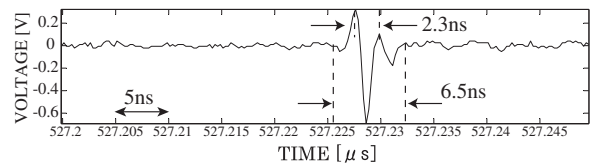


(b) 300MHz band.

Fig. 3: The frequency characteristics of receiving systems.



(a) The entire waveform.



(b) The expanded waveform.

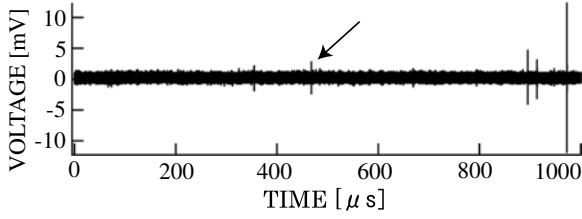
Fig. 4: An experimental result of hypervelocity impact at 2GHz band.

current according to an equivalent model by an electric small dipole [2].

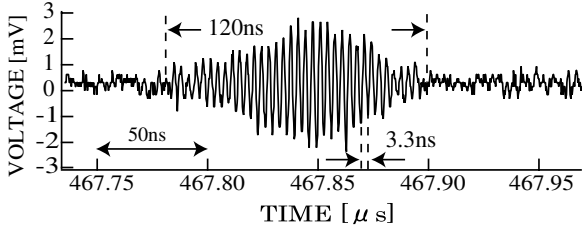
The radiation electric field E_{θ} is given by,

$$E_{\theta} = jA(r, \theta) \frac{I(\omega) k^2}{\sqrt{2} \omega} e^{-jkr} \quad (1)$$

where E_{θ} is the vertical component of field, j is imaginary unit, $A(r, \theta)$ is the constant determined by experimental condition, ω is angular frequency, $I(\omega)$ is the complex spectrum of spark discharge current $i(t)$, $k(= \omega/c)$ is the wave number, c is the light velocity, r is the propagated distance, and θ is the angle made by the line connecting each charge and the propagation direction. Also, the spark discharge current $i(t)$



(a) The entire waveform.



(b) The expanded waveform.

Fig. 5: An experimental result of hypervelocity impact at 300MHz band.

is given by [4],

$$i(t) = \frac{3\sqrt{3}}{2} \cdot \frac{\exp(3\sqrt{3}t/\tau)}{[1 + \exp(3\sqrt{3}t/\tau)]^{1.5}} \quad (2)$$

where $\tau(=2\text{ns})$ is the nominal duration time. Lastly, the antenna reception voltage spectrum $V_i(\omega)$ can be given by [5],

$$V_i(\omega) = \gamma E_\theta = j A_0 \omega I(\omega) \quad (3)$$

where γ is the conversion factor between the antenna reception voltage and the electric field. The propagation delay is ignored. In addition, A_0 is given by,

$$A_0 \equiv \frac{\gamma}{\sqrt{2}c^2} A(r = R, \theta = \theta_0) \quad (4)$$

where R and θ_0 is the distance and the angle determined by the experimental condition, respectively.

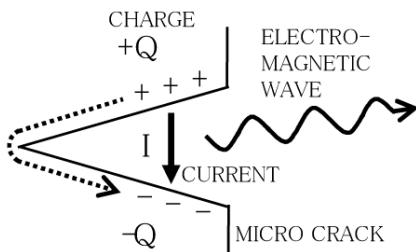


Fig. 6: The microwave emission model due to the discharge across the microcrack.

B. Analytical methods

The numerical calculation procedure is explained in the order of each receiving device shown in Fig.2. Procedures are on the basis of Eq.(3) at 2GHz band.

- (1) Multiplying V_i by the transfer function $H(\omega)$. $H(\omega)$ is the characteristics of LNA and BPF. $H(\omega)$ is assumed to be a rectangular shape shown in Fig.3(a) or a gaussian shape. In the case of a gaussian shape, RF band is spectrum space of 3dB relaxation.
- (2) Calculating Inverse Fourier Transform of (1).
- (3) Multiplying (2) by $\cos(\omega_{LO}t - \phi)$ to obtain IF band. ω_{LO} is local angular frequency, and ϕ is phase.
- (4) Calculating Fourier Transform of (3).
- (5) Multiplying (4) by the transfer function $G(\omega)$. $G(\omega)$ is the characteristics of IF Amp. and assumed to be a rectangular shape.
- (6) Calculating Inverse Fourier Transform of (5).
- (7) Taking real part of (6).

At 300MHz band, only procedures (1), (2), (7) are necessary since mixer and IF Amp. are not included.

C. Analytical results and discussions

The signal at 2GHz band is processed using the rectangular filter which is indicated in Fig.3(a) by the word "Band". The analytical result is shown in Fig.7. Also, the value of pulse width is shown in Table 1 to compare experimental results with analytical ones. It turns out that the waveform changes because of the phase ϕ of the mixer. The waveform similar to the experimental result is obtained in the case of $\phi = (-5/8)\pi$ in comparison to Fig.4(b).

The waveform resembles AM signal since the waveform is composed of the envelope with the width of inverse number of band width and the carrier of center frequency. The period of center frequency of analytical result is 2.4ns and corresponds with experimental one. But, the width of envelope is much longer than 6.5ns and the whole length of pulse cannot be seen. This is because the rectangular filter shown in Fig.3(a) narrows the frequency characteristics

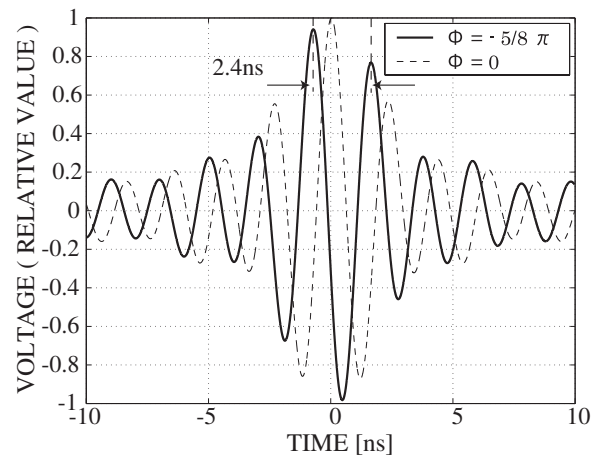


Fig. 7: An analytical result by the rectangular filter in the receiving system for 2GHz band.

Next, we use a gaussian filter at 2GHz band which approximates the measured curve shown in Fig.3(a). The analytical

result is shown in Fig.8. The period of center frequency is 2.1ns and corresponds with the experimental result. The width of envelope is 8.7ns and approximately corresponds with the experimental result. This is because the width of envelope becomes shorter as the band width of the gaussian filter becomes effectively broader than the rectangular filter.

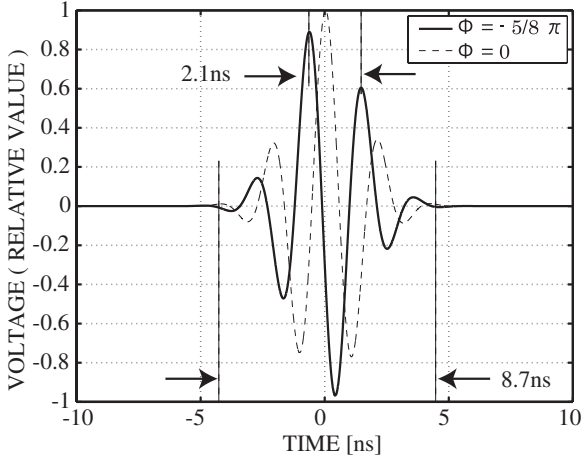


Fig. 8: The analytical result by the gaussian filter in the receiving system for 2GHz band.

At 300MHz band, the analytical result is shown in Fig.9. The shape of waveform like AM corresponds to the experimental one. Also, the period of center frequency is 3.3ns, and the width of envelope is 120ns. So, these results correspond with analytical ones.

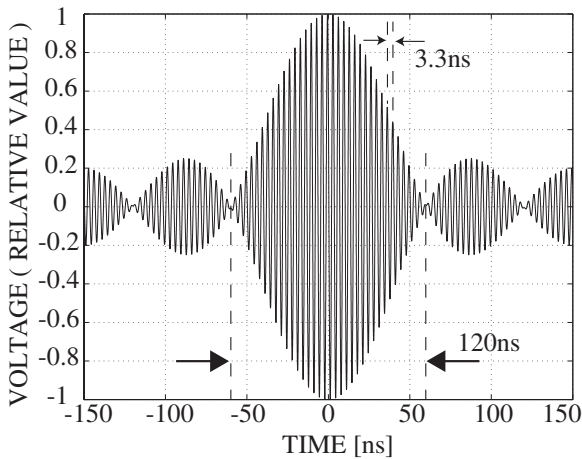


Fig. 9: An analytical result in the receiving system for 300MHz band.

From Fig.8 and Fig.9, it is indicated that this hypothesis of mechanism is valid as the mechanism of microwave emissions.

TABLE 1: THE PERIOD OF CENTER FREQUENCY AND THE WIDTH OF ENVELOPE.

Frequency band	Experiment		Analysis	
	Period	Envelope	Period	Envelope
2GHz (Rectangular)	2.3ns	6.5ns	2.4ns	-
2GHz (Gaussian)			2.1ns	8.7ns
300MHz	3.3ns	120ns	3.3ns	120ns

4. SPECTRAL ANALYSIS

A. Analytical method

First, a pulse is extracted from the entire waveform with the extraction time T_s . A reason for extraction is to reduce the effect of noise. If the complex spectrum is calculated over the entire measurement time $T_m = 1000\mu s$, the characteristics of spectrum cannot be seen due to the noise because radiative time is much shorter than the entire time T_m . The extraction time T_s is 50 [ns] at 2GHz band, 250 [ns] at 300MHz band, respectively. The extraction time T_s is determined so as to be longer than one pulse.

Second, the waveform is multiplied by window function. Since it is desirable that the value of both edge of waveform is zero because of the following procedure due to FFT, the waveform is adjusted by multiplying by Hanning window $h(t)$. Hanning window $h(t)$ is given by,

$$h(t) = 0.5 \left(1 + \cos \frac{2\pi}{T_s} t \right) \quad (5)$$

Third, the complex spectrum $V_s(\omega)$ is calculated by FFT.

Lastly, the amplitude $P(\omega)$ and the phase $\phi(\omega)$ of spectrum are calculated by equations given by,

$$P(\omega) = 10 \log_{10} |V_s(\omega)|^2 \quad (6)$$

$$\phi(\omega) = \tan^{-1} \frac{\text{Im}[V_s(\omega)]}{\text{Re}[V_s(\omega)]} \quad (7)$$

where Re and Im are operators to take real and imaginary part, respectively. In addition, the domain of definition of $\phi[\text{deg}]$ is $-90 < \phi < 90$.

B. Analytical results and discussions

The spectral amplitude at 2GHz band is shown in Fig.10(a). The frequency is expressed in IF band. It is found that the amplitude is nearly flat ranging in several hundreds MHz although the decline of about 5dB can be seen around 200MHz (equivalent to 2150MHz in RF band).

The phase of spectrum at 2GHz band is shown in Fig.10(b). The phase is locally linear but has phase jump of 180 degree. This phase jump of 180 degree is corrected. The 180 degree is subtracted from each phase values after phase jump. As a result, the phase characteristics becomes almost linear.

Variable a , defined as the gradient of phase characteristics, is $-1.29[\text{deg}/\text{MHz}]$. The gradient a is required to be corrected because the gradient decreases by $2\pi t_0$ where t_0 is the lag time from the center of window in Fig.4(b). The center is the time $527.225\mu s$ within $T_s=50ns$. If t_0 is 4ns, the correction

value a_{cor} is estimated: $a_{cor} = -(-2\pi t_0) = 1.44[\text{deg}/\text{MHz}]$. Consequently, this value has to be added to the gradient as follows.

$$a' = a + a_{cor} = 0.15 [\text{deg}/\text{MHz}] \quad (8)$$

So, it is found that the phase have coherency at 2GHz band since the value of gradient is almost zero and the phase is almost constant.

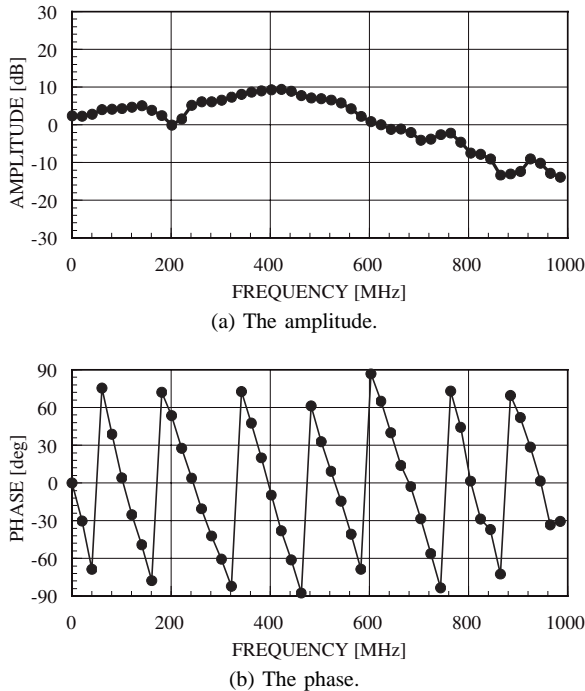


Fig. 10: Analytical results of an experimental waveform at 2GHz band. The frequency is expressed in IF band.

The spectral amplitude at 300MHz band is shown in Fig.11(a). It is found that the amplitude is almost similar to the frequency characteristics shown in Fig.3(b). It is indicated to be nearly flat around the band.

The phase of spectrum at 300MHz band is shown in Fig.11(b). The phase is almost the same values against frequency within the band. So, the phase has coherency.

It is indicated from results of 2GHz and 300MHz band that emissions have coherency at both frequency bands. As a conclusion, it is thought that the mechanism of microwave emissions is not the one which has random phases such as Bremsstrahlung radiation by a group of plasma particles.

5. CONCLUSION

The followings in relation to microwave emissions accompanying hypervelocity impacts are obtained at 2GHz and 300MHz band:

- (1) Output waveform analysis is carried out on the basis of the microcrack model of microwave emissions to be compared with experimental waveform. Receiving

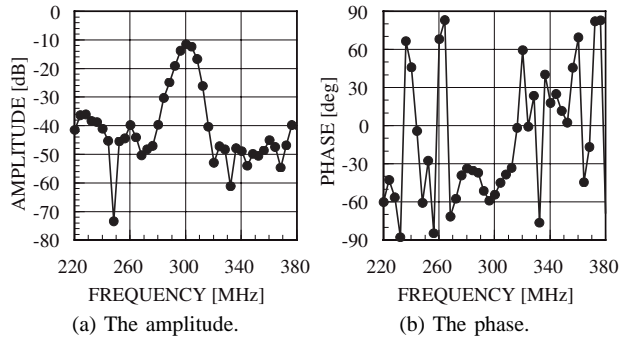


Fig. 11: Analytical results of an experimental waveform at 300MHz band.

systems can be simulated by using reception voltage spectrum V_i

- (2) At 2GHz band, it is found that output waveforms change by the phase of local signal because of use of mixer in the heterodyne receiving system.
- (3) Analytical results at 2GHz band by the gaussian filter and 300MHz band accord with experimental ones in terms of the pulse shape and width.
- (4) It is indicated that microcrack model used for the analysis is valid as the mechanism.
- (5) Spectral analysis of experimental waveforms shows that the amplitude is nearly flat ranging in several hundreds MHz and the phase is also nearly flat and has coherency within each frequency band.
- (6) The mechanism which includes random phases is not suitable to this phenomenon.

REFERENCES

- [1] T.Takano, Y.Murotani, K.Maki, T.Toda, A. Fujiwara, S.Hasegawa, A.Yamori and H.Yano, "Microwave emission due to hypervelocity impacts and its correlation with mechanical destruction", J. Appl. Phys., vol.92, no.9, pp.5550-5554 (2002)
- [2] K. Maki, T. Takano, A. Fujiwara and A. Yamori, "Radio-wave emission due to hypervelocity impacts in relation to optical observation and projectile speed", Advances in Space Research, vol.34, pp.1085-1089 (2004)
- [3] K. Maki, T. Takano, E. Soma, K. Ishii, S. Yoshida, M. Nakatani, "Observation of Microwave Emissions in Rock Fracture under Pressure", Zisin (Journal of the Seismological Society of Japan), 58(4), 375-384 (2006)
- [4] O. Fujiwara, "An analytical approach to model indirect effect caused by electrostatic discharge", IEICE Trans. Commun., vol.E79-B, no.4, pp.483-489 (1996)
- [5] K. Maki, E. Soma, T. Takano, A. Fujiwara, and A. Yamori, "Dependence of microwave emissions from hypervelocity impacts on the target material", J. Appl. Phys., vol.97, 104911 (2005)
- [6] MATLAB, Copyright 1984-2000, The MathWorks, Inc.